

# MCRB for Parameter Estimation from One-Bit Quantized and Oversampled Measurements

Nadav E. Rosenthal, *Student Member, IEEE*, and Joseph Tabrikian, *Fellow, IEEE*

**Abstract**—One-bit quantization has garnered significant attention in recent years for various signal processing and communication applications. Estimating model parameters from one-bit quantized data can be challenging, particularly when the quantization process is explicitly accounted for in the estimator. In many cases, the estimator disregards quantization effects, leading to model misspecification. Consequently, estimation errors arise from both quantization and misspecification. Traditional performance bounds, such as the Cramér-Rao bound (CRB), fail to capture the impact of misspecification on estimation performance. To address this limitation, we derive the misspecified CRB (MCRB) for parameter estimation in a quantized data model consisting of a signal component in additive Gaussian noise. We apply this bound to direction-of-arrival estimation using quantized measurements from a sensor array and to frequency estimation with oversampled quantized data. The simulations show that the MCRB is asymptotically achieved by the mean-squared-error of the misspecified maximum-likelihood estimator. Our results demonstrate that, unlike in finely quantized scenarios, oversampling can significantly enhance the estimation performance in the presence of misspecified one-bit quantized measurements.

**Index Terms**—Quantization, performance bounds, mean-squared-error, misspecified Cramér-Rao bound (MCRB).

## I. INTRODUCTION

Quantization is commonly used in communications and digital signal processing. For example, in array signal processing, analog-to-digital converters (ADC) [1], [2] convert the analog signal received from the antennas into discrete values, which can be stored and processed by a digital computer. Reducing the number of bits required to represent the collected data decreases the storage and bandwidth requirements, which are essential for data compression and transmission.

Implementations of one-bit quantization in signal processing and communication systems, which are inexpensive and involve low energy consumption, have been vastly investigated [3]–[14]. Recent works have investigated the effects of one-bit quantization on channel estimation [15]–[18], frequency estimation [19], and direction-of-arrival (DOA) estimation [20]. Many system designs have been suggested based on one-bit quantized data in multiple-input multiple-output (MIMO) and massive MIMO problems [21]–[25].

Quantization introduces signal distortion which leads to system performance degradation [26]. In addition, signal processing algorithms that are aware of the quantization become complex and involve higher computational complexity, which

may increase the cost as well as higher energy consumption. In [20], a minimum-variance distortionless response (MVDR) estimator for DOA estimation based on reconstructed covariance matrix of one-bit quantized measurements was proposed. However, this estimator collapses for high signal-to-noise ratios (SNRs), because the reconstructed covariance matrix becomes singular. Other estimators based on empirical methods for evaluating the orthant probabilities have been suggested [20], but they require Monte-Carlo simulations and lack closed-form expressions. Channel estimation in massive MIMO systems based on low-resolution is also challenging due to the nonlinear distortion caused by quantization [4]. Several channel estimators have been proposed based on deep neural networks [27]–[31].

An appealing and simple approach for processing one-bit quantized data is to implement conventional estimators that ignore the effect of quantization. The question that arises is: what is the expected performance when conventional algorithms that disregard quantization, are applied to one-bit quantized data? In this case, estimation errors are due to both quantization effect and model misspecification.

The effect of one-bit quantization on parameter estimation can be investigated via estimation performance bounds. Performance bounds provide important tools in signal processing, since they serve as a benchmark for performance evaluation of estimators and are useful for system design. The most common performance bound in the non-Bayesian framework is the Cramér-Rao bound (CRB) [32], [33]. Its popularity stems from its simplicity and asymptotic attainability.

Derivation of lower bounds for estimation performance with one-bit quantized measurements has been challenging. For example, an explicit formula for the CRB for frequency estimation performance does not exist, and the CRB for large-enough signal-to-noise ratio (SNR) was investigated [19]. For the DOA estimation problem investigated in [20], the CRB was derived explicitly only for a two-sensor array. The CRB and Fisher information for channel estimation for oversampled quantized measurements cannot be analytically derived [34], because the derivations require evaluation and explicit formulas for orthant probabilities [35]–[37]. Thus, approximations for the CRB were proposed based on Fisher information lower bounds [34], [38]–[40].

The CRB assumes perfect model specification by the estimator, thus it cannot consider the influence of misspecification on the estimation performance. Therefore, it is unable to predict the expected estimation performance of conventional estimators implemented on one-bit quantized data.

In [41]–[43] the asymptotic properties of the maximum-likelihood (ML) estimator were investigated under misspecified models where the data samples are statistically indepen-

This research was partially supported by THE ISRAEL SCIENCE FOUNDATION (grant No. 2493/23).

The authors are with the School of Electrical and Computer Engineering, Ben-Gurion University of the Negev, Beer-Sheva 84105, Israel (e-mail: rosenthn@post.bgu.ac.il; joseph@bgu.ac.il)

dent. The misspecified CRB (MCRB) was derived in [44] as an extension of the CRB to misspecified scenarios. Continuing this theory, the effects of model misspecification on the mean-squared error (MSE) of the ML in the asymptotic region were studied in [45], [46]. An important overview on misspecified parameter estimation can be found in [47].

Many works have investigated the advantages of oversampling quantized data on information rates and channel capacity [34], [48]–[55]. It is well-known that in case of  $\infty$ -bit quantization, oversampling a bandlimited signal beyond the Nyquist rate does not improve the estimation or signal recovery performance [56]. However, in [52], [53], it was shown that oversampling a bandlimited signal with additive white Gaussian noise (AWGN) and one-bit quantization outperforms Nyquist sampling in terms of capacity per unit-cost and achievable rate at high SNR. The effect of oversampling one-bit quantized data on estimation performance is unknown. Therefore, a tool for analysis of such problems may be very helpful in signal processing theory and applications.

In this paper, the effects of model misspecification due to ignoring one-bit quantization are investigated. We derive the MCRB and the expected bias of estimators that ignore one-bit quantization. Using the derived MCRB, we analyze the expected performance of estimators implemented on one-bit quantized data. Moreover, we use the MCRB in order to show how the estimation performance can be improved by oversampling of one-bit quantized data. The computational complexity of the estimation procedure with fine quantization and one-bit measurements are compared in terms of computational complexity. We consider the problems of DOA and frequency estimation using one-bit quantized measurements, and evaluate the expected bias and the MCRB, compared to the misspecified ML estimator. In the problem of DOA estimation, the derived MCRB is compared with the CRB based on one-bit quantized measurements. Moreover, the MCRB identifies scenarios where misspecified quantization heavily degrades the performance. In the problem of frequency estimation, oversampling of the quantized data is shown to improve the estimation performance. A conference version of this work with some preliminary results is expected to appear in [57]. This paper includes several extensions, such as derivation of MCRB for colored noise, performance analysis of oversampling for the problem of frequency estimation through the MCRB, and computational complexity analysis of the ML estimator with misspecified one-bit quantized measurements.

The main contributions of this paper are:

- Derivation of the MCRB for predicting the expected performance of estimators that ignore one-bit quantization. Its final form is more explicit and easy to evaluate than the CRB for one-bit quantized measurements.
- Application of the derived MCRB for the problems of DOA estimation and frequency estimation with one-bit quantized measurements.
- Exploration of oversampling effects on estimation performance with one-bit quantized measurements. It is shown that unlike the case of  $\infty$ -bit quantization, oversampling of one-bit quantized data can improve the expected estimation performance.

Throughout this paper, the following notations are used. Boldface lowercase and boldface uppercase letters are used to denote vectors and matrices, respectively. Unbold letters of either lowercase or uppercase are used for scalars. Superscripts  $T$ ,  $H$ , and  $*$  stand for transpose, conjugate transpose, and conjugation operations, respectively. The real and imaginary parts of a variable  $b \in \mathbb{C}$  are denoted by  $\Re(b)$  or  $b_R$ , and  $\Im(b)$  or  $b_I$ , respectively. The gradient of a scalar  $b$  with respect to (w.r.t.)  $\mathbf{a} \in \mathbb{R}^K$  is a column vector, whose  $j$ -th element is defined as  $\left[\frac{db(\mathbf{a})}{d\mathbf{a}}\right]_j \triangleq \frac{\partial b(\mathbf{a})}{\partial c_j} \Big|_{\mathbf{c}=\mathbf{a}}$ . Given a vector  $\mathbf{b}$ , its derivative w.r.t.  $\mathbf{a}$  is a matrix whose  $j, k$ -th entry is defined as  $\left[\frac{d\mathbf{b}}{d\mathbf{a}}\right]_{j,k} \triangleq \frac{\partial b_j(\mathbf{c})}{\partial c_k} \Big|_{\mathbf{c}=\mathbf{a}}$ . The first and second-order derivatives of a function vector  $\mathbf{b}(\mathbf{c})$  w.r.t. the scalar  $c$  are denoted by  $\dot{\mathbf{b}}(c) \triangleq \frac{d\mathbf{b}(c)}{dc}$  and  $\ddot{\mathbf{b}}(c) \triangleq \frac{d^2\mathbf{b}(c)}{dc^2}$ , respectively. The notation  $\mathbf{A} \succeq \mathbf{B}$  implies that  $\mathbf{A} - \mathbf{B}$  is a positive-semidefinite matrix, where  $\mathbf{A}$  and  $\mathbf{B}$  are symmetric matrices of the same size.  $\det(\mathbf{A})$  and  $\text{tr}(\mathbf{A})$  stand for the determinant and trace of the matrix  $\mathbf{A}$ , respectively.  $\text{Diag}(\mathbf{a})$  is a diagonal matrix whose diagonal elements are the entries of the vector  $\mathbf{a}$ . Column vectors of size  $N$ , whose entries are equal to 0 or 1 are denoted by  $\mathbf{0}_N$  and  $\mathbf{1}_N$ , respectively, and the identity matrix of size  $N \times N$  is denoted by  $\mathbf{I}_N$ .

This paper is organized as follows. Section II presents the model for one-bit quantized measurements. In Section III the MCRB is derived for estimation procedures that ignore the one-bit quantization. The derivation is extended to the case of over-sampled quantized data models. In Section IV, ML estimation based on fine quantization and one-bit measurements are presented and compared in terms of computational cost. Simulation results are presented in Section V. Finally, our conclusions are summarized in Section VI.

## II. ONE-BIT QUANTIZED DATA MODEL

Consider the problem of estimating the vector parameter  $\boldsymbol{\theta} \in \Omega_{\boldsymbol{\theta}} \subseteq \mathbb{R}^M$  from a nonlinear model with additive noise. The data model before quantization is given by

$$\mathbf{x} = \mathbf{s}(\boldsymbol{\theta}) + \mathbf{v}, \quad (1)$$

where  $\mathbf{v} \in \mathbb{C}^N$  is complex Gaussian noise with zero mean and covariance matrix  $\mathbf{R}$ , and  $\mathbf{s} : \Omega_{\boldsymbol{\theta}} \rightarrow \mathbb{C}^N$  is the signal function vector. The elements of the covariance matrix  $\mathbf{R}$  are denoted by

$$[\mathbf{R}]_{n,m} \triangleq \begin{cases} \sigma_n^2, & n = m \\ \rho_{n,m}, & n \neq m \end{cases}, \quad n, m = 1, \dots, N. \quad (2)$$

The real and imaginary parts of the measurements are one-bit quantized:

$$z_n = \text{sign}(x_{n,R}) + j \cdot \text{sign}(x_{n,I}), \quad n = 1, \dots, N, \quad (3)$$

where

$$\text{sign}(x) \triangleq \begin{cases} +1, & x \geq 0 \\ -1, & x < 0 \end{cases}. \quad (4)$$

The probability mass function (PMF) of the real and imaginary parts of the quantized measurements (3) can be derived as follows [16]:

$$p_{z_n,R;\boldsymbol{\theta}}(z_{n,R};\boldsymbol{\theta}) = Q(z_{n,R}q_{n,R}(\boldsymbol{\theta})), \quad z_{n,R} \in \{-1, 1\}, \quad (5)$$

and

$$p_{z_{n,I};\boldsymbol{\theta}}(z_{n,I};\boldsymbol{\theta}) = Q(z_{n,I}q_{n,I}(\boldsymbol{\theta})), \quad z_{n,I} \in \{-1, 1\}, \quad (6)$$

where

$$q_n(\boldsymbol{\theta}) \triangleq -\frac{s_n(\boldsymbol{\theta})}{\frac{\sigma_n}{\sqrt{2}}}, \quad n = 1, \dots, N, \quad (7)$$

$s_n(\boldsymbol{\theta})$  is the  $n$ -th signal function, and

$$Q(x) \triangleq \frac{1}{\sqrt{2\pi}} \int_x^\infty e^{-\frac{u^2}{2}} du \quad (8)$$

is the standard Q-function. Let the series of events  $\{\omega_n^{(k_n)}\}_{n=1}^N$ ,  $k_n = 0, \dots, 3$ , specify the possible values of the elements of  $\mathbf{z} \triangleq [z_1, \dots, z_N]^T$ :

$$\omega_n^{(k_n)} \triangleq \begin{cases} z_n = -1 - j, & \text{if } k_n = 0 \\ z_n = -1 + j, & \text{if } k_n = 1 \\ z_n = 1 - j, & \text{if } k_n = 2 \\ z_n = 1 + j, & \text{if } k_n = 3 \end{cases} \\ = \begin{cases} x_{n,R} < 0 \cap x_{n,I} < 0, & \text{if } k_n = 0 \\ x_{n,R} < 0 \cap x_{n,I} \geq 0, & \text{if } k_n = 1 \\ x_{n,R} \geq 0 \cap x_{n,I} < 0, & \text{if } k_n = 2 \\ x_{n,R} \geq 0 \cap x_{n,I} \geq 0, & \text{if } k_n = 3 \end{cases}, n = 1, \dots, N, \quad (9)$$

where the second equality in (9) is obtained by the quantization operators in (3). The PMFs of the quantized measurement vector,  $\mathbf{z}$ , are given by using (9):

$$p_{\mathbf{z};\boldsymbol{\theta}}(\mathbf{z};\boldsymbol{\theta}) \triangleq \text{Prob}\left(\cap_{n=1}^N \omega_n^{(k_n)}\right), \quad \{k_n\}_{n=1}^N \in \{0, 1, 2, 3\}. \quad (10)$$

The set of  $4^N$  probabilities defined in (10) is a set of non-centered orthant probability functions (multivariate version of the Q-function) of the vector composed of the real and imaginary parts of the elements of  $\mathbf{x}$  [35]–[37]. Unfortunately, closed-form expressions for the orthant probabilities in (10) do not exist. Therefore, derivation of a procedure for estimation of  $\boldsymbol{\theta}$  based on the true PMFs in (10) is complex and impossible in the general setting.

Instead of using a complex estimation algorithm that accounts for the quantization, a simple approach for processing one-bit quantized data is to implement a conventional estimator that ignores the effect of quantization. The assumed model  $f(\mathbf{z};\boldsymbol{\theta})$  ignores the quantization operator and assumes the vector  $\mathbf{v}$  is complex white Gaussian with covariance matrix  $\sigma^2 \mathbf{I}_N$ . Under this model, the distribution of  $\mathbf{z}$  is given by

$$f: \mathbf{z} \sim \mathcal{N}^C(\mathbf{s}(\boldsymbol{\theta}), \sigma^2 \mathbf{I}_N). \quad (11)$$

In Section III, we derive the MCRB for estimation procedures that ignore one-bit quantization. The derived MCRB provides a useful analysis tool which can serve for both performance evaluation and system design.

### III. MCRB DERIVATION

In this section, we consider a basic model which is common in many signal processing applications, such as frequency or DOA estimation. This model is a special case of the model

presented in the previous section, where the signal function vector is given by

$$\mathbf{s}(\boldsymbol{\theta}) \triangleq \beta \mathbf{a}(\varphi), \quad (12)$$

where  $\boldsymbol{\theta} \triangleq [\varphi, \beta_R, \beta_I]^T$ ,  $\varphi \in \Omega_\varphi \subseteq \mathbb{R}$  is a deterministic and unknown parameter-of-interest, and  $\beta \in \mathbb{C}$  is deterministic unknown complex amplitude. The function  $\mathbf{a}: \Omega_\varphi \rightarrow \mathbb{C}^N$  is assumed to be known and satisfy  $\|\mathbf{a}(\varphi)\|^2 = 1$  and  $\dot{\mathbf{a}}^H(\varphi)\mathbf{a}(\varphi) = 0$ ,  $\forall \varphi \in \Omega_\varphi$ . We ought to evaluate the quantization impact on the expected estimation performance of conventional estimators that disregard the quantization, in terms of bias and expected covariance [45].

#### A. Estimation Bias and Pseudo-True Parameter

For an estimator  $\hat{\boldsymbol{\theta}}(\mathbf{z})$  the mean bias is defined by:

$$\mathbf{b}(\hat{\boldsymbol{\theta}}, \boldsymbol{\theta}) \triangleq \mathbb{E}[\hat{\boldsymbol{\theta}}(\mathbf{z})] - \boldsymbol{\theta}, \quad (13)$$

while the property of misspecified (MS) unbiasedness [47] is defined by  $\mathbb{E}[\hat{\boldsymbol{\theta}}(\mathbf{z})] = \boldsymbol{\theta}_0$ , where  $\boldsymbol{\theta}_0$  is the pseudo-true parameter vector given by [44]

$$\boldsymbol{\theta}_0 \triangleq \arg \max_{\boldsymbol{\theta}' \in \Omega_\theta} \mathbb{E}[\log f(\mathbf{z}; \boldsymbol{\theta}')]. \quad (14)$$

The expectations in (13) and (14), as well as throughout the paper, are taken w.r.t. the true PMF, and true parameter  $\boldsymbol{\theta}$ . For cases that the true and assumed distributions are continuous, the pseudo-true parameter is alternatively defined by the parameter that minimizes the Kullback-Leibler divergence (KLD) between the true and assumed distributions [58]. The misspecified ML estimator is known to be asymptotically MS-unbiased. In this subsection, the estimation mean-bias in (13) is investigated for estimators  $\hat{\boldsymbol{\theta}}(\mathbf{z})$  that are MS-unbiased and satisfy

$$\mathbf{b}(\hat{\boldsymbol{\theta}}, \boldsymbol{\theta}) = \boldsymbol{\theta}_0 - \boldsymbol{\theta}. \quad (15)$$

The assumed log-likelihood at the parameter vector  $\boldsymbol{\theta}'$  is given by using (11) and (12):

$$\log f(\mathbf{z}; \boldsymbol{\theta}') = -N \log(\pi \sigma^2) - \frac{\|\mathbf{z} - \beta' \mathbf{a}(\varphi')\|^2}{\sigma^2}, \quad (16)$$

where  $\boldsymbol{\theta}' = [\varphi', \beta'_R, \beta'_I]^T$ . By substituting (16) into the right hand side (r.h.s.) of (14), removing the terms that are independent of  $\boldsymbol{\theta}'$  and using  $\|\mathbf{a}(\varphi')\|^2 = 1$ , one obtains

$$\boldsymbol{\theta}_0 = \arg \max_{\boldsymbol{\theta}' \in \Omega_\theta} \left[ 2\Re(\beta' \boldsymbol{\mu}^H(\boldsymbol{\theta}) \mathbf{a}(\varphi')) - |\beta'|^2 \right], \quad (17)$$

where  $\boldsymbol{\mu}(\boldsymbol{\theta}) \triangleq \mathbb{E}[\mathbf{z}]$  is derived in (66) and (67) in Appendix A and depends on both  $\varphi$  and  $\beta$ . Maximizing the expression in (17) w.r.t.  $\boldsymbol{\theta}'$  yields the pseudo-true parameter vector

$$\boldsymbol{\theta}_0 = [\varphi_0, \beta_{0,R}, \beta_{0,I}]^T, \quad (18)$$

where the pseudo-true parameter-of-interest is

$$\varphi_0 = \arg \max_{\varphi'} |MAF(\varphi', \boldsymbol{\theta})|, \quad (19)$$

in which the misspecified ambiguity function (MAF) is defined by

$$MAF(\varphi', \boldsymbol{\theta}) \triangleq \frac{\mathbf{a}^H(\varphi')\boldsymbol{\mu}(\boldsymbol{\theta})}{\max_{\varphi'} |\mathbf{a}^H(\varphi')\boldsymbol{\mu}(\boldsymbol{\theta})|}, \quad (20)$$

and the pseudo-true complex amplitude is

$$\beta_0 = \mathbf{a}^H(\varphi_0)\boldsymbol{\mu}(\boldsymbol{\theta}). \quad (21)$$

Note that the pseudo-true parameter-of-interest in (19) is derived by the parameter that maximizes the absolute of MAF in (20), which is the correlation between the quantized measurements expectation,  $\boldsymbol{\mu}(\boldsymbol{\theta})$ , and the function,  $\mathbf{a}(\cdot)$ . Examining the MAF, we note that it depends on  $\boldsymbol{\theta}$  through  $\boldsymbol{\mu}(\boldsymbol{\theta})$ . Specifically, it depends on the true complex amplitude  $\beta$  by a nonlinear function. For the unquantized model in (1), the ambiguity function (AF) can be defined by  $AF(\varphi', \varphi) \triangleq \frac{\mathbf{a}^H(\varphi')\mathbf{a}(\varphi)}{\|\mathbf{a}(\varphi')\|\|\mathbf{a}(\varphi)\|}$  (see [59]), which obtains its maximum at  $\varphi' = \varphi$ . Notice that the AF is independent on  $\beta$ . By substitution of (19) in the r.h.s. of (15) and evaluating its first element, one obtains the estimation bias of the parameter-of-interest,  $\varphi$ ,

$$b_1(\hat{\boldsymbol{\theta}}, \boldsymbol{\theta}) = \arg \max_{\varphi'} |MAF(\varphi', \boldsymbol{\theta})| - \varphi. \quad (22)$$

### B. MSE Performance and MCRB

In this subsection, the MCRB is derived to investigate the expected MSE performance for a MS-unbiased estimator  $\hat{\boldsymbol{\theta}}(\mathbf{z})$ , derived from the assumed model in (11). The MCRB for estimation of  $\boldsymbol{\theta}$  from the quantized measurements  $\mathbf{z}$  is given by [47]

$$\text{MCRB}(\boldsymbol{\theta}) \triangleq \mathbf{A}_{\boldsymbol{\theta}_0}^{-1} \mathbf{B}_{\boldsymbol{\theta}_0} \mathbf{A}_{\boldsymbol{\theta}_0}^{-1}, \quad (23)$$

where the matrices  $\mathbf{B}_{\boldsymbol{\theta}_0}$  and  $\mathbf{A}_{\boldsymbol{\theta}_0}$  are defined by

$$\mathbf{B}_{\boldsymbol{\theta}_0} \triangleq \mathbb{E} [\mathbf{d}(\mathbf{z}, \boldsymbol{\theta}_0) \mathbf{d}^T(\mathbf{z}, \boldsymbol{\theta}_0)], \quad (24)$$

$$\mathbf{A}_{\boldsymbol{\theta}_0} \triangleq \mathbb{E} [\mathbf{H}(\mathbf{z}, \boldsymbol{\theta}_0)], \quad (25)$$

and the gradient and Hessian of the assumed log-likelihood w.r.t.  $\boldsymbol{\theta}$  at  $\boldsymbol{\theta}_0$  are given by

$$\mathbf{d}(\mathbf{z}, \boldsymbol{\theta}_0) \triangleq \frac{\partial \log f(\mathbf{z}; \boldsymbol{\theta}_0)}{\partial \boldsymbol{\theta}} \quad (26)$$

and

$$\mathbf{H}(\mathbf{z}, \boldsymbol{\theta}_0) \triangleq \frac{\partial^2 \log f(\mathbf{z}; \boldsymbol{\theta}_0)}{\partial \boldsymbol{\theta} \partial \boldsymbol{\theta}^T}, \quad (27)$$

respectively. By substitution of (16) at (18) in (26) and (27), followed by few calculations, we obtain

$$\mathbf{d}(\mathbf{z}, \boldsymbol{\theta}_0) = \frac{2}{\sigma^2} \begin{bmatrix} d_1 \\ d_{2,R} \\ d_{2,I} \end{bmatrix}, \quad (28)$$

and

$$\mathbf{H}(\mathbf{z}, \boldsymbol{\theta}_0) = \frac{2}{\sigma^2} \begin{bmatrix} h_1 & h_{2,R} & h_{2,I} \\ h_{2,R} & -1 & 0 \\ h_{2,I} & 0 & -1 \end{bmatrix}, \quad (29)$$

where  $d_1 = \Re(\mathbf{z}^H \dot{\mathbf{a}}(\varphi_0)\beta_0)$ ,  $d_2 = \mathbf{a}^H(\varphi_0)\mathbf{z} - \beta_0$ ,  $h_1 \triangleq \Re(\mathbf{z}^H \ddot{\mathbf{a}}(\varphi_0)\beta_0)$  and  $h_2 \triangleq \dot{\mathbf{a}}^H(\varphi_0)\mathbf{z}$ . By substituting (28) and (29) into (24) and (25), respectively, and using (65) from Appendix A, we obtain after a few lines of algebra,

$$\mathbf{B}_{\boldsymbol{\theta}_0} = \frac{2}{\sigma^4} \begin{bmatrix} L_1 & L_{2,R} & L_{2,I} \\ L_{2,R} & L_5 & L_4 \\ L_{2,I} & L_4 & L_6 \end{bmatrix} \quad (30)$$

and

$$\mathbf{A}_{\boldsymbol{\theta}_0} = \frac{2}{\sigma^2} \begin{bmatrix} J_1 & J_{2,R} & J_{2,I} \\ J_{2,R} & -1 & 0 \\ J_{2,I} & 0 & -1 \end{bmatrix}, \quad (31)$$

where the elements of (30) and (31) are

$$\begin{aligned} J_1 &\triangleq \mathbb{E}[h_1] = \Re(\boldsymbol{\mu}^H(\boldsymbol{\theta})\ddot{\mathbf{a}}(\varphi_0)\beta_0), \\ J_2 &\triangleq \mathbb{E}[h_2] = \dot{\mathbf{a}}^H(\varphi_0)\boldsymbol{\mu}(\boldsymbol{\theta}), \\ L_1 &\triangleq \Re(\beta_0^2 \dot{\mathbf{a}}^T(\varphi_0)\mathbf{P}^* \dot{\mathbf{a}}(\varphi_0)) + |\beta_0|^2 \dot{\mathbf{a}}^H(\varphi_0)\mathbf{M}\dot{\mathbf{a}}(\varphi_0), \\ L_2 &\triangleq \beta_0^* \dot{\mathbf{a}}^H(\varphi_0)\mathbf{P}\mathbf{a}^*(\varphi_0) \\ &\quad + \beta_0 (\mathbf{a}^H(\varphi_0)\mathbf{M}\dot{\mathbf{a}}(\varphi_0) - 2\Re(J_2\beta_0^*)), \\ L_3 &\triangleq \mathbf{a}^H(\varphi_0)\mathbf{P}\mathbf{a}^*(\varphi_0), \\ L_4 &\triangleq L_{3,I} - 2\beta_{0,R}\beta_{0,I}, \\ L_5 &\triangleq L_{3,R} + \mathbf{a}^H(\varphi_0)\mathbf{M}\mathbf{a}(\varphi_0) - 2(\beta_{0,R})^2, \\ L_6 &\triangleq -L_{3,R} + \mathbf{a}^H(\varphi_0)\mathbf{M}\mathbf{a}(\varphi_0) - 2(\beta_{0,I})^2, \end{aligned} \quad (32)$$

and the second-order moment and second-order pseudo-moment matrices of the quantized measurements vector,  $\mathbf{z}$ , are denoted by  $\mathbf{M} \triangleq \mathbb{E}[\mathbf{z}\mathbf{z}^H]$  and  $\mathbf{P} \triangleq \mathbb{E}[\mathbf{z}\mathbf{z}^T]$ , respectively. Substitution of (31) and (30) in (23) followed by few simple calculations form the MCRB for the parameter-of-interest,  $\varphi$ , with one-bit quantized data

$$\begin{aligned} [\text{MCRB}(\boldsymbol{\theta})]_{1,1} &= \\ &= \frac{L_1 + 2\Re(J_2 L_2^*) + L_6 J_{2,I}^2 + L_5 J_{2,R}^2 + 2L_4 J_{2,I} J_{2,R}}{2(|J_2|^2 + J_1)^2}. \end{aligned} \quad (33)$$

Finally, the corresponding bound on the MSE of the estimator  $\hat{\varphi}(\mathbf{z})$  of  $\varphi$  is given by using (22) and (33) [47]

$$\text{MSE}(\hat{\varphi}(\mathbf{z})) \triangleq \mathbb{E}[(\hat{\varphi}(\mathbf{z}) - \varphi)^2] \geq [\text{MCRB}(\boldsymbol{\theta})]_{1,1} + b_1^2(\hat{\boldsymbol{\theta}}, \boldsymbol{\theta}). \quad (34)$$

For evaluating the MSE bound in (34), explicit expressions for the matrices  $\mathbf{M}$  and  $\mathbf{P}$  are required. In Subsection III-C we derive the MCRB for oversampled one-bit quantized measurements. Oversampling in a frequency larger than the Nyquist rate results in colored noise. Thus, in the following subsections, we analyze the elements of the matrices  $\mathbf{M}$  and  $\mathbf{P}$  for the general case of colored noise,  $\mathbf{v}$ , with covariance matrix  $\mathbf{R}$ , and the special case where the noise,  $\mathbf{v}$ , is AWGN.

#### 1) MCRB for One-Bit Quantized Data in Colored Noise:

The elements  $[\mathbf{M}]_{i,l}$  and  $[\mathbf{P}]_{i,l}$  are given by

$$[\mathbf{M}]_{i,l} \triangleq \mathbb{E}[z_i z_l^*], \quad i, l = 1, \dots, N \quad (35)$$

and

$$[\mathbf{P}]_{i,l} \triangleq \mathbb{E}[z_i z_l], \quad i, l = 1, \dots, N, \quad (36)$$

respectively. Evaluating (35) and (36) for  $i = l$  while using the statistics of quantized random variables in (65)-(68) in Appendix A, yields

$$[\mathbf{M}]_{i,i} = \mathbb{E}[|z_i|^2] = 2 \quad (37)$$

and

$$[\mathbf{P}]_{i,i} = \mathbb{E}[z_i^2] = 2j \cdot \mu_{i,R}(\boldsymbol{\theta}) \mu_{i,I}(\boldsymbol{\theta}). \quad (38)$$

Evaluating the elements (35) and (36) for  $i \neq l$  gives

$$[\mathbf{M}]_{i,l} = \sum_{\substack{z_i, z_l \in \{\pm 1 \pm j\}, \\ k_i, k_l = 0, \dots, 3}} P_{i,l}^{(k_i, k_l)} z_i z_l^*, \quad (39)$$

and

$$[\mathbf{P}]_{i,l} = \sum_{\substack{z_i, z_l \in \{\pm 1 \pm j\}, \\ k_i, k_l = 0, \dots, 3}} P_{i,l}^{(k_i, k_l)} z_i z_l, \quad (40)$$

where the PMFs of  $\mathbf{z}_{i,l} \triangleq [z_i, z_l]^T$  are denoted by  $P_{i,l}^{(k_i, k_l)}$ ,  $k_i, k_l = 0, \dots, 3$  and obtained from the quantization rule (3) and the events described in (9) for  $z_i$  and  $z_l$ :

$$P_{i,l}^{(k_i, k_l)} = \text{Prob}\left(\omega_i^{(k_i)} \cap \omega_l^{(k_l)}\right), \quad k_i, k_l = 0, \dots, 3, \quad (41)$$

$$i, l = 1, \dots, N.$$

Let the vector  $\mathbf{x}_{i,l}$  be defined as

$$\mathbf{x}_{i,l} \triangleq [x_{i,R}, x_{i,I}, x_{l,R}, x_{l,I}]^T, \quad i, l = 1, \dots, N. \quad (42)$$

According to the model in (1),  $\mathbf{x}_{i,l} \sim \mathcal{N}(\mathbf{u}_{i,l}, \mathbf{C}_{i,l})$ , where

$$\mathbf{u}_{i,l} \triangleq [s_{i,R}(\boldsymbol{\theta}), s_{i,I}(\boldsymbol{\theta}), s_{l,R}(\boldsymbol{\theta}), s_{l,I}(\boldsymbol{\theta})]^T \quad (43)$$

and

$$\mathbf{C}_{i,l} \triangleq \frac{1}{2} \begin{bmatrix} \sigma_i^2 & 0 & \rho_{i,l} & 0 \\ 0 & \sigma_i^2 & 0 & \rho_{i,l} \\ \rho_{i,l} & 0 & \sigma_l^2 & 0 \\ 0 & \rho_{i,l} & 0 & \sigma_l^2 \end{bmatrix} \quad (44)$$

are the expectation vector and the covariance matrix of  $\mathbf{x}_{i,l}$ , respectively, where (44) is obtained from properties of the circularly symmetric complex Gaussian distribution with covariance matrix elements in (2). The set of 16 probabilities defined in (41) is the quadrivariate set of non-centered orthonormal probability functions of  $\mathbf{x}_{i,l}$  [35]–[37], [60], [61]. Evaluation of the set in (41) requires computing the four dimensional integrals

$$P_{i,l}^{(k_i, k_l)} = \int_{B_{i,l}^{(k_i, k_l)}} \phi(\mathbf{x}_{i,l}, \mathbf{u}_{i,l}, \mathbf{C}_{i,l}) d\mathbf{x}_{i,l}, \quad (45)$$

$$k_i, k_l = 0, \dots, 3,$$

where  $\phi(\mathbf{x}, \mathbf{u}, \mathbf{C})$  is the quadrivariate Gaussian probability density function (PDF) and the integration region  $B_{i,l}^{(k_i, k_l)}$  is defined by

$$B_{i,l}^{(k_i, k_l)} \triangleq \{\mathbf{x}_{i,l} \in \mathbb{R}^4 | \omega_i^{(k_i)} \cap \omega_l^{(k_l)}\}. \quad (46)$$

Although there is no closed-form expression for the integral in the r.h.s. of (45), numerical integration methods like Quasi Monte-Carlo methods [35], [62] can be applied to approximate it. Substitution of the approximations of (45) in (39) and (40) gives the elements  $[\mathbf{M}]_{i,l}$  and  $[\mathbf{P}]_{i,l}$  for  $i \neq l$ ,  $i, l = 1, \dots, N$ , respectively.

## 2) MCRB for One-Bit Quantized Data in AWGN:

For the special case of AWGN where  $\mathbf{R} = \sigma^2 \mathbf{I}_N$ , the covariance matrix in (44) resides to

$$\mathbf{C}_{i,l} = \frac{1}{2} \sigma^2 \mathbf{I}_4, \quad i, l = 1, \dots, N. \quad (47)$$

Therefore, the elements of  $\mathbf{x}_{i,l}$  for  $i \neq l$  are statistically independent, since  $\mathbf{x}_{i,l}$  is Gaussian, and the probability in (45) can be expressed by the product of marginal probabilities of  $\mathbf{x}_{i,l}$ . After few lines of algebra, it can be shown that

$$P_{i,l}^{(k_i, k_l)} = p_{z_{i,R}; \boldsymbol{\theta}}(z_{i,R}; \boldsymbol{\theta}) p_{z_{i,I}; \boldsymbol{\theta}}(z_{i,I}; \boldsymbol{\theta}) \\ \times p_{z_{l,R}; \boldsymbol{\theta}}(z_{l,R}; \boldsymbol{\theta}) p_{z_{l,I}; \boldsymbol{\theta}}(z_{l,I}; \boldsymbol{\theta}), \quad (48)$$

$$z_i, z_l \in \{\pm 1 \pm j\},$$

By substituting (48) into (39) and (40) one obtains

$$[\mathbf{M}]_{i,l} = \sum_{z_i \in \{\pm 1 \pm j\}} p_{z_{i,R}; \boldsymbol{\theta}}(z_{i,R}; \boldsymbol{\theta}) p_{z_{i,I}; \boldsymbol{\theta}}(z_{i,I}; \boldsymbol{\theta}) z_i \\ \times \sum_{z_l \in \{\pm 1 \pm j\}} p_{z_{l,R}; \boldsymbol{\theta}}(z_{l,R}; \boldsymbol{\theta}) p_{z_{l,I}; \boldsymbol{\theta}}(z_{l,I}; \boldsymbol{\theta}) z_l^* \\ = \mathbb{E}[z_i] \mathbb{E}[z_l^*] = \mu_i(\boldsymbol{\theta}) \mu_l^*(\boldsymbol{\theta}), \quad i \neq l, \quad (49)$$

and

$$[\mathbf{P}]_{i,l} = \mathbb{E}[z_i] \mathbb{E}[z_l] = \mu_i(\boldsymbol{\theta}) \mu_l(\boldsymbol{\theta}), \quad i \neq l. \quad (50)$$

The diagonal elements of  $\mathbf{M}$  and  $\mathbf{P}$  are given by (37) and (38), respectively.

## C. MCRB for Oversampled Quantized Data

The derived MCRB can be used not only for performance evaluation in the case of one-bit quantization, but also to evaluate and analyze potential performance improvement through oversampling. Nyquist rate sampling of a deterministic band-limited signal with AWGN and low-pass filter, followed by one-bit quantization is expected to produce statistically independent observations. However, statistical independence is not preserved in the case of oversampling. An overview on sampling continuous-time signals can be found in [56]. The covariance matrix elements of a band-limited continuous time signal in AWGN are [38]

$$[\mathbf{R}]_{n,m} = \sigma^2 \cdot \text{sinc}(2BT_s(n-m)), \quad n, m = 1, \dots, N, \quad (51)$$

where  $T_s$  and  $f_s = \frac{1}{T_s}$  are the sampling time interval and frequency, respectively,  $B$  is the bandwidth of the signal, and

$$\text{sinc}(x) \triangleq \frac{\sin(\pi x)}{\pi x}. \quad (52)$$

If the sampling frequency is exactly equal to the Nyquist rate  $f_s = 2B$ , then (51) resides to  $\mathbf{R} = \sigma^2 \mathbf{I}_N$  and the noise

vector  $\mathbf{v}$  is white. In order to obtain the MCRB for parameter estimation with oversampled quantized measurements where  $f_s > 2B$ , the elements of the matrices  $\mathbf{M}$  and  $\mathbf{P}$  in (35) and (36) should be evaluated with the covariance matrix in (51). Substitution of the resulting  $\mathbf{M}$  and  $\mathbf{P}$  matrices in (32), followed by their substitution in (33) and (34) gives the MCRB and MSE bound for estimation with oversampled quantized measurements, respectively.

In Section V, we evaluate the MSE bounds for one-bit quantized data and show that oversampling may partially compensate for the lost information due to quantization. A similar trade-off exists in terms of computational complexity. While processing of one-bit quantized data is simpler, increasing the sampling rate may involve higher amount of computations. The question that can be raised is whether the computational complexity of the conventional estimator with quantized measurements is reduced compared to the conventional estimator with finite number of bits per measurement. In the next section, the estimation procedures for the models in (1) and (3) are presented, and their computational costs are discussed.

#### IV. COMPUTATIONAL COMPLEXITY OF ONE-BIT QUANTIZED AND OVERSAMPLED MEASUREMENTS

In this section, we analyze the computational complexity of the misspecified ML estimator based on one-bit and fine quantization measurements in terms of the number of real operations: multiplication, addition, or subtraction,  $C_{op}$ . The algorithm based on one-bit measurements is shown to be more efficient than the fine quantization algorithm, in terms of computational complexity. Moreover, the influence of oversampling on the computational complexity is presented.

The ML estimator under the assumed model in (11) with non-quantized measurements is given by [63]

$$\hat{\varphi}(\mathbf{x}) \triangleq \arg \max_{\varphi'} \left| c(\mathbf{a}(\varphi'), \mathbf{x}) \right|^2, \quad (53)$$

where the correlator  $c: \mathbb{C}^N \times \mathbb{C}^N \rightarrow \mathbb{C}$  is defined by

$$c(\mathbf{h}, \mathbf{u}) \triangleq \mathbf{h}^H \mathbf{u}. \quad (54)$$

The same estimator is used in the quantized case where the input is substituted by  $\mathbf{z}$ :  $\hat{\varphi}(\mathbf{z})$ .

**Proposition 1.** Assume the misspecified ML estimators based on fine quantization and one-bit quantized measurements are evaluated with grid parameter  $\varphi'$  and  $K$  possible values of  $\varphi'$ . Let  $C_{\mathbf{z}}$  and  $C_{\mathbf{x}}$  define the computational complexity of the estimator with one-bit and fine quantization, respectively. Then, the reduction in the computational complexity for using one-bit measurements is

$$\lim_{N \rightarrow \infty} \frac{C_{\mathbf{z}}}{C_{\mathbf{x}}} = \frac{1}{4} \quad (55)$$

*Proof.* The proof appears in Appendix B. ■

For the case of over-sampled quantized measurements  $\mathbf{z}$ , the computational complexity increases by the oversampling factor  $U \triangleq \frac{f_s}{2B}$ . Thus, the computational complexity using quantized measurements with oversampling factor  $U$ ,

increases by a factor of  $\frac{U}{4}$ . Accordingly, processing of over-sampled quantized data with  $U < 4$  is computationally more efficient than processing fine-quantized data at Nyquist rate.

#### V. SIMULATIONS

In this section, the expected performance of misspecified one-bit quantized measurements in two signal processing applications is investigated via the MCRB and mean-bias. In Subsection V-A the problem of DOA estimation using a sensor array is considered, and in Subsection V-B the problem of frequency estimation is addressed. The MCRB is used to evaluate the expected performance for oversampled one-bit quantized data.

##### A. DOA Estimation

In the problem of DOA estimation of a narrowband far-field source, the measurement model before quantization can be described by (1) and (12), where  $\mathbf{a}(\varphi)$  is the steering vector of direction  $\varphi \in \Omega_\varphi \subseteq (-\frac{\pi}{2}, \frac{\pi}{2})$  and  $\beta \in \mathbb{C}$  is deterministic unknown complex amplitude. Consider a uniform linear array (ULA) of  $N = 16$  sensors with half a wavelength inter-element spacing. Thus, the  $n$ -th element of the steering vector  $\mathbf{a}(\varphi)$  is given by

$$a_n(\varphi) = \frac{1}{\sqrt{N}} \exp \left[ j\pi \left( n - \frac{N+1}{2} \right) \sin \varphi \right]. \quad (56)$$

According to the discussion in Section III-C, the noise vector  $\mathbf{v}$  is white Gaussian. The SNR is defined by  $SNR \triangleq \frac{|\beta|^2}{\sigma_v^2}$ . Figs. 1a and 1b depict the AF and MAF, respectively, versus spatial frequency  $u = \sin \varphi$  for real  $\beta$ , and  $SNR = 30\text{dB}$ . The MAF that considers model misspecification due to one-bit quantization presents several distinguished properties:

- Distorted mainlobes in width and shape, compared to the AF.
- Sidelobe distance from the mainlobe and their heights depend on  $\sin \varphi$ .
- Three large-valued lobe patterns that cross  $\varphi'$  grid and intersect with the mainlobe.

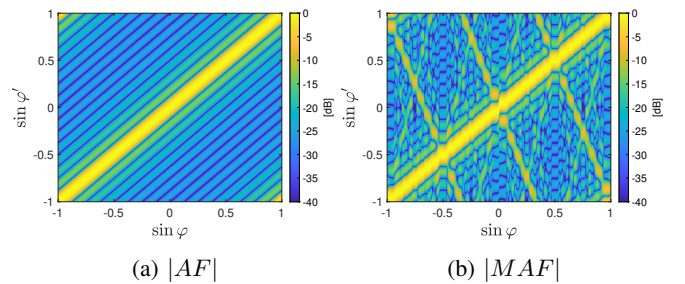


Fig. 1: Comparison between perfectly specified and misspecified ambiguity functions for DOA estimation with ULA of  $N = 16$  sensors, complex amplitude phase  $\angle \beta = 0^\circ$ , and  $SNR = 30\text{dB}$ .

Fig. 2 depicts the absolute estimation bias given in (22) versus DOA for several SNR's. For  $SNR = 10\text{dB}$  the estimation bias is relatively small and it increases as the

SNR grows. For example, large estimation bias of  $9^\circ$  and  $1.8^\circ$  at  $SNR = 30\text{dB}$  correspond to distorted mainlobes and intersection points in Fig. 1b. In those DOAs the pseudo-true DOA, which is the parameter that maximizes the MAF along  $\sin \varphi'$  grid, is influenced by the distorted mainlobes. The root-

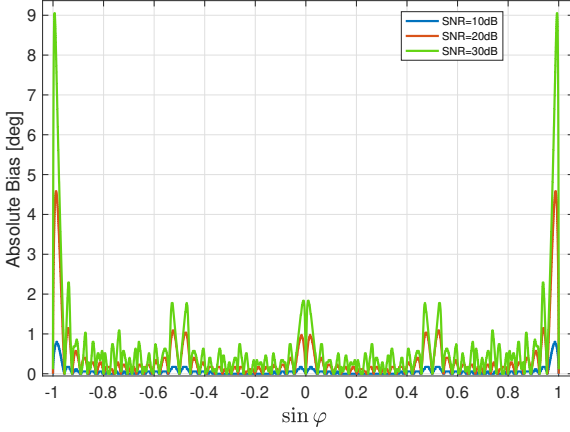


Fig. 2: Absolute estimation bias versus DOA for several SNR's with ULA of  $N = 16$  sensors, and complex amplitude phase  $\angle\beta = 0^\circ$ .

MSE (RMSE) performance of the misspecified ML estimator  $\hat{\varphi}(\mathbf{z})$  is presented in Fig. 3 along with the MSE bound (34) (denoted as MCRB) for DOA  $\varphi = 0^\circ$ , and several complex amplitude phases  $\angle\beta$  versus SNR. Moreover, the CRB for the quantized model (3) is derived and presented similarly to [16], [19] to obtain

$$CRB(\varphi) = \left[ \mathbf{J}^{-1}(\boldsymbol{\theta}) \right]_{1,1}, \quad (57)$$

where the Fisher information matrix (FIM) is given by

$$\mathbf{J}(\boldsymbol{\theta}) = \sum_{n=1}^N \left[ \psi(q_{n,R}(\boldsymbol{\theta})) \frac{ds_{n,R}(\boldsymbol{\theta})}{d\boldsymbol{\theta}} \left( \frac{ds_{n,R}(\boldsymbol{\theta})}{d\boldsymbol{\theta}} \right)^T + \psi(q_{n,I}(\boldsymbol{\theta})) \frac{ds_{n,I}(\boldsymbol{\theta})}{d\boldsymbol{\theta}} \left( \frac{ds_{n,I}(\boldsymbol{\theta})}{d\boldsymbol{\theta}} \right)^T \right], \quad (58)$$

in which the function  $\psi(\cdot)$  is defined by

$$\psi(q) \triangleq \frac{\exp[-q^2]}{\sigma^2 \pi [Q(q) - Q^2(q)]}. \quad (59)$$

Fig. 3 shows that the misspecified ML estimator is bounded by (34), and its RMSE approaches it for high SNR's. The MCRB for complex amplitude phase  $\angle\beta = 0^\circ$  converges to a constant value at high SNRs. This phenomenon and the dependency on complex amplitude phase  $\angle\beta$  is explained as follows. Substituting  $\varphi = 0^\circ$ ,  $\angle\beta = 0^\circ$ , and (12) in (1), and evaluating the real and imaginary parts of its  $n$ -th entry result in

$$\begin{aligned} x_{n,R} &= \beta [\mathbf{a}(0)]_n + v_{n,R}, \\ x_{n,I} &= v_{n,I}, \end{aligned} \quad (60)$$

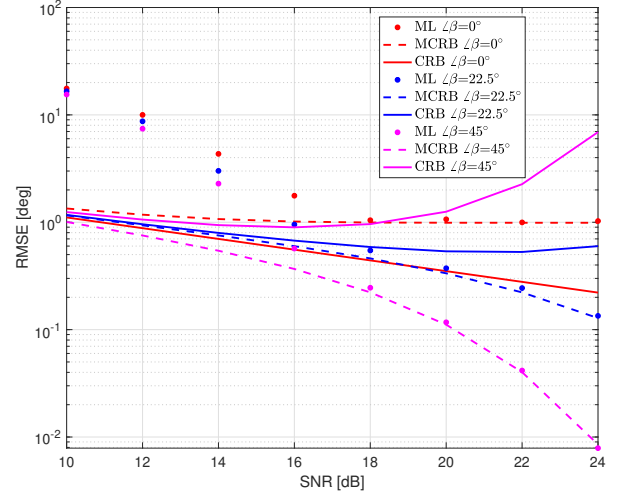


Fig. 3: RMSE of misspecified ML, MSE bound, and CRB versus SNR for several complex amplitude phases, ULA of  $N = 16$  sensors, and  $\varphi = 0^\circ$ .

since  $\beta [\mathbf{a}(0)]_n$  is real. Substituting (60) in (3) gives the quantized measurements

$$z_n = \text{sign} \left( \beta [\mathbf{a}(0)]_n + v_{n,R} \right) + j \cdot \text{sign} (v_{n,I}), \quad (61)$$

as the complex amplitude and DOA terms are present in the real part and absent in the imaginary part. Thus, the imaginary part of (61) includes only noise, and according to (6), it is symmetric Bernoulli-distributed. As SNR increases in (61), the real part converges to 1. Evaluating the possible phases of the measurement  $z_n$  gives  $\angle z_n \in \{-45^\circ, 45^\circ\}$ , where each one of the two values is obtained with probability (w.p.) 0.5. Since the DOA information is induced in the measurement phases, by the uncertainty in the phase  $\angle z_n$  one obtains constant RMSE performance as shown in Fig. 3.

For other complex amplitude phases like  $\angle\beta = 45^\circ$ , following the same derivation in (60)-(61) concludes that the real and imaginary parts of  $z_n$  include both signal and noise parts. Thus, as SNR increases, the measurement phase  $\angle z_n$  converges to a specific value w.p. 1, and the RMSE reduces, as shown in Fig. 3. Comparing the MCRB for the misspecified scenario where the quantization is ignored to the quantized CRB gives an interesting insight. For some complex amplitude phases like  $\angle\beta = 45^\circ$ , using conventional algorithms which ignore the quantization, decreases the estimation errors compared to quantized estimation, while for other phases like  $\angle\beta = 0^\circ$  the estimation errors are increased. The MCRB and CRB differences can be explained by considering the classes of estimators that the bounds apply to. The MCRB applies to MS-unbiased estimators, while the CRB applies to unbiased estimators. The class of MS-unbiased estimators are generally mean-biased in the perfectly specified sense. Thus, their RMSE performance is not bounded by the CRB, and may be lower than the CRB. To emphasize this phenomenon, Fig. 4 depicts the CRB and MCRB including bias versus DOA and complex amplitude phase  $\angle\beta$  for  $SNR = 20\text{dB}$ .



Notice that both bounds depend on complex amplitude phase, are symmetric around  $\angle\beta = 45^\circ$  and periodic with period  $\angle\beta = 90^\circ$  due to the symmetry of the real and imaginary parts of  $\mathbf{z}$ . For example, for DOAs  $\varphi = 0^\circ, -30^\circ, 30^\circ$ , the MCRB and CRB increase or decrease as function of  $\angle\beta$ . For these DOAs, the CRB reaches significantly higher values than the MCRB for most complex amplitude phases. Thus, surprisingly, ignoring the quantization in estimation can decrease the estimation errors.

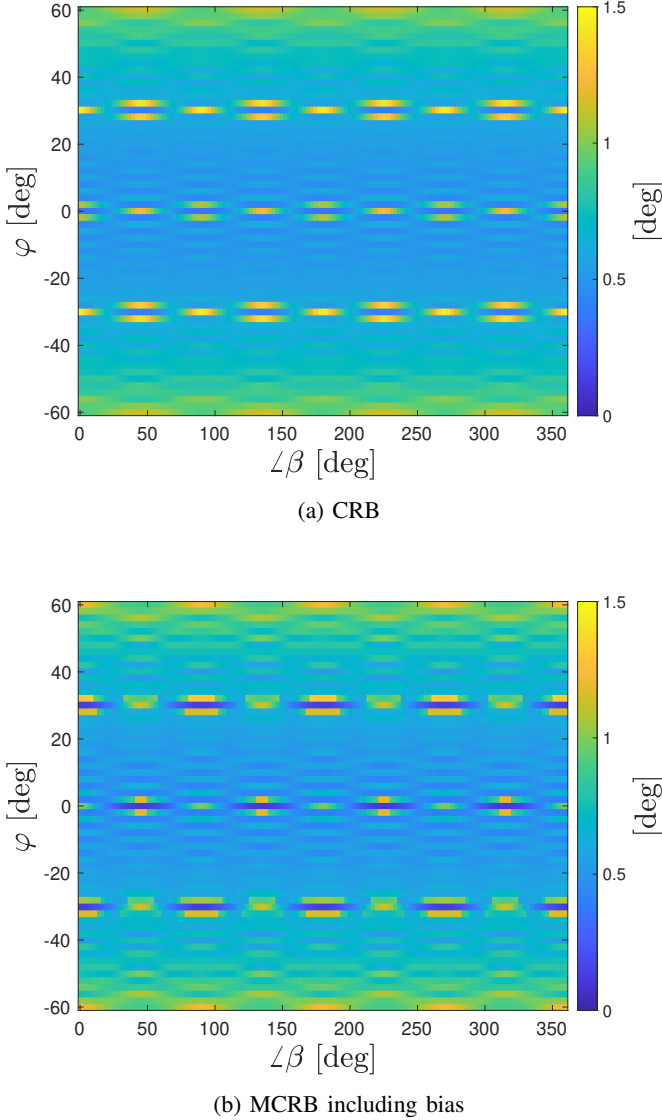


Fig. 4: Comparison of the CRB and the MCRB including bias contribution versus DOA and complex amplitude phase  $\angle\beta$  for ULA of  $N = 16$  sensors, and  $SNR = 20$ dB.

### B. Oversampling in Frequency Estimation

In the problem of frequency estimation, the measurements model before quantization can be described by (1) and (12), where the elements of the vector  $\mathbf{a}(\varphi)$  are

$$[\mathbf{a}(\varphi)]_n = \frac{1}{\sqrt{N}} \exp[j2\pi\varphi t_n], \quad n = 1, \dots, N, \quad (62)$$

$\varphi \in \Omega_\varphi \subseteq [0, 2.5\text{KHz})$  is the frequency, and  $\{t_n\}$  are the time samples

$$t_n = t_1 + (n-1)T_s, \quad n = 1, \dots, N. \quad (63)$$

The time samples are symmetric around 0 such that (s.t.)  $t_1 = -\frac{T}{2}$ ,  $t_N = \frac{T}{2}$  where  $T$  is the observation interval, and the assumption  $\dot{\mathbf{a}}^H(\varphi)\mathbf{a}(\varphi) = 0$ ,  $\forall \varphi \in \Omega_\varphi$  is satisfied. As the signal frequency is unknown, we specify that the ideal low-pass filter bandwidth is  $B = 2.5\text{KHz}$ . The following figures illustrate the estimation performance of one-bit quantized data after oversampling. We denote the oversampling factor by  $U \triangleq \frac{f_s}{B}$ .

Figs. 5a and 5b depict the AF and MAF, respectively, versus frequency  $\varphi$  for sampling rate  $f_s = 2.5\text{KHz}$ , observation interval  $T = 8\text{msec}$ , real  $\beta$ , and SNR per sample of 7dB. The MAF for frequency estimation that considers the misspecification due to one-bit quantization presents similar properties to the MAF for DOA estimation in Fig. 1b. Figs. 6a and 6b depict the MAFs for oversampled signal with oversampling factor  $U$ . Compared to the MAF in Fig. 5b, as the oversampling factor  $U$  increases, the distortions in the MAF that result from the one-bit quantization decay and vanish. For example, the three sidelobe patterns in Fig. 5b reduce to one sidelobe in Fig. 6a, and none in 6b. Thus, oversampling reduces the effects of quantization on the MAF. Recalling the correlator  $c(\mathbf{a}(\varphi'), \mathbf{z})$  and evaluating its expectation gives

$$\mathbb{E}[c(\mathbf{a}(\varphi'), \mathbf{z})] = \mathbf{a}^H(\varphi')\boldsymbol{\mu}(\boldsymbol{\theta}) = C \cdot \text{MAF}(\varphi', \boldsymbol{\theta}), \quad (64)$$

where  $C$  is a constant in  $\varphi'$ . As mentioned above, the MAF includes distortions and sidelobe patterns, which their influence is reduced with increased oversampling factor  $U$ . Thus, oversampling reduces the misspecified ML  $\hat{\varphi}(\mathbf{z})$  sensitivity to sidelobes and distortions caused by quantization, and improves the estimation accuracy.

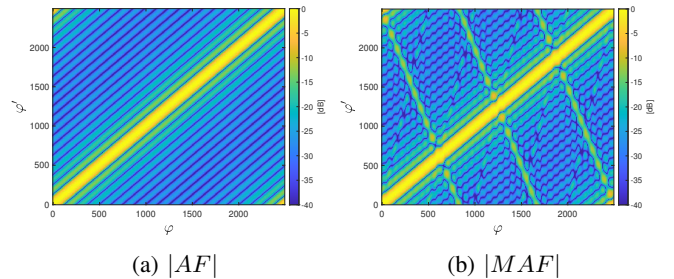


Fig. 5: Comparison of ambiguity functions for frequency estimation for sampling rate  $f_s = 2.5\text{KHz}$ , observation interval  $T = 8\text{msec}$ , complex amplitude phase  $\angle\beta = 0^\circ$ , and  $SNR = 7\text{dB}$  per sample.

The RMSEs of the ML estimator with fine-quantized measurements (53) are presented in Fig. 7 versus SNR per sample for several oversampling factors  $U$ , with frequency  $\varphi = 1\text{KHz}$ , observation interval  $T = 4\text{msec}$ , and complex amplitude phase  $\angle\beta = 60^\circ$ . It can be seen that the RMSEs of the three estimators coincide in the asymptotic region. Thus, oversampling of fine-quantized band-limited measurements does not reduce the RMSE for large SNRs.



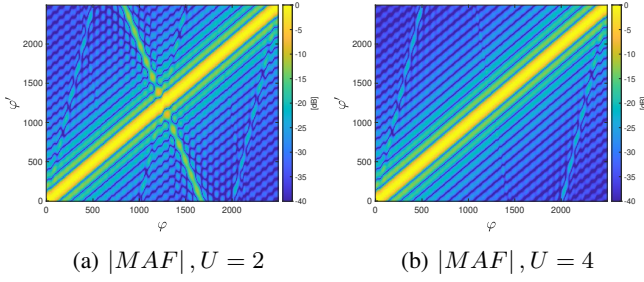


Fig. 6: Comparison of MAFs for oversampled frequency estimation for sampling rate  $f_s = 2.5\text{KHz} \cdot U$ , observation interval  $T = 8\text{msec}$ , complex amplitude phase  $\angle\beta = 0^\circ$ , and  $\text{SNR} = 7\text{dB}$  per sample.

This result is expected, as oversampling does not improve band-limited signal reconstruction for sampling frequencies above the Nyquist rate. The RMSEs of the ML estimator with

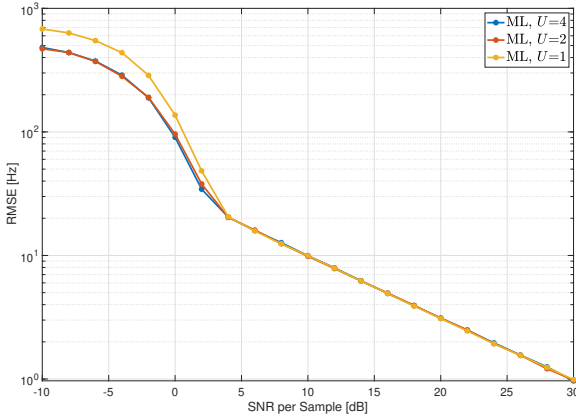


Fig. 7: RMSE of the ML estimator with fine quantization measurements versus SNR for sampling rate  $f_s = 2.5\text{KHz} \cdot U$  and oversampling factors  $U$ , frequency  $\varphi = 1\text{KHz}$ , observation interval  $T = 4\text{msec}$ , and complex amplitude phase  $\angle\beta = 60^\circ$ .

fine quantization measurements,  $\hat{\varphi}(\mathbf{x})$ , and with misspecified quantized measurements,  $\hat{\varphi}(\mathbf{z})$ , are presented in Fig. 8 versus SNR per sample for several oversampling factors  $U$ , with frequency  $\varphi = 1\text{KHz}$ , observation interval  $T = 4\text{msec}$ , and complex amplitude phase  $\angle\beta = 60^\circ$ . The RMSE of the ML estimator in (53) is presented only for  $U = 1$ , because Fig. 7 illustrated that oversampling of fine quantization measurements does not reduce the RMSE. Moreover, the MSE bound for the misspecified estimators due to the quantization is depicted for several oversampling factors in Fig. 8. It can be observed that the RMSE of the misspecified ML  $\hat{\varphi}(\mathbf{z})$  reduces significantly as the oversampling factor  $U$  increases for high SNRs. The RMSE performance of the misspecified ML without oversampling ( $U = 1$ ) results in large bias for high SNRs. When the oversampling factor increases to  $U = 4$ , the improvement in RMSE performance of the misspecified ML is most noticeable, with smallest expected bias and RMSE lower than that of the ML that relies on fine quantization measurements. The influence of oversampling on estimation performance is veri-

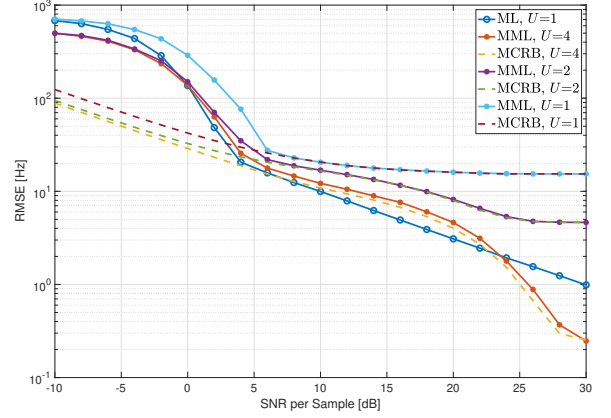


Fig. 8: RMSEs of the ML estimator with fine quantization, misspecified ML estimator of the quantized measurements, and MSE bound versus SNR for sampling rate  $f_s = 2.5\text{KHz} \cdot U$  and oversampling factors  $U$ , with frequency  $\varphi = 1\text{KHz}$ , observation interval  $T = 4\text{msec}$ , and complex amplitude phase  $\angle\beta = 60^\circ$ .

fied by the MSE bound, which predicts the asymptotic RMSE of the misspecified ML. Thus, oversampling can significantly improve the estimation performance when the measurements are quantized, even outperforming the estimation performance with fine-quantized measurements. One might ask how using oversampled and quantized measurements can improve the RMSE performance compared to using fine quantization measurements. The misspecified ML estimator based on quantized measurements belongs to the class of MS-unbiased estimators, which are generally biased in the perfectly specified case. Thus, the RMSE of the misspecified ML estimator is not bounded by the conventional CRB based on fine quantization measurements, and can be lower than the CRB. Recalling the discussion in Section IV, oversampling with factors  $U = 2, 4$  and estimation with the one-bit quantization is more efficient or has similar computational costs compared to estimation based on fine quantization measurements. Thus, the estimation procedure  $\hat{\varphi}(\mathbf{z})$  after oversampling can gain better estimation performance compared to the estimation procedure (53) without significant additional computational costs.

In order to investigate the influence of oversampling on estimation performance, the MSE bound (34) is presented in Fig. 9 versus complex amplitude phase  $\angle\beta$  for several oversampling factors  $U$ , with frequency  $\varphi = 1\text{KHz}$ , and observation interval  $T = 4\text{msec}$ . For most complex amplitude phases  $\angle\beta$ , increasing the oversampling factor  $U$  reduces the MSE performance, where significant reductions appear for oversampling factors  $U = 2, 4$ . However, for complex amplitude phases  $\angle\beta = 45^\circ, 135^\circ, 225^\circ, 315^\circ$ , the MSE performance for  $U = 1$  is relatively low. Therefore, MSE performance strongly depends on the complex amplitude phase  $\angle\beta$  as well.

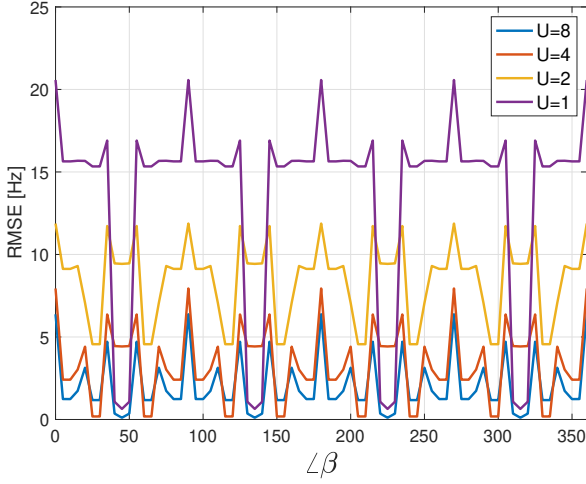


Fig. 9: MSE bound versus complex amplitude phase  $\angle\beta$ , SNR=30dB per sample, for sampling rate  $f_s = 2.5\text{KHz}$  ·  $U$  and oversampling factors  $U$ , frequency  $\varphi = 1\text{KHz}$ , and observation interval  $T = 4\text{msec}$ .

## VI. CONCLUSION

In this paper, we considered the problem of parameter estimation with misspecified one-bit quantized measurements. Instead of regarding the quantization in the estimation procedure, which results in a complex estimator, one may ignore the quantization and use conventional estimation procedures, introducing misspecification in the model. In order to investigate the estimation performance, the MCRB and expected bias are derived for quantized measurements with AWGN or colored noise. A comparison of the computational cost of estimation procedures with fine quantization and one-bit measurements is given. Test cases of DOA and frequency estimation are presented to investigate the influence of misspecification due to quantization. For the problem of DOA estimation, the RMSE performance of the misspecified ML estimator and the MCRB depend on DOA, SNR, and complex amplitude phase. For the problem of frequency estimation, the influence of oversampling on quantized measurements is investigated. It is shown that oversampling reduces the effects of quantization on estimation performance, and can result in better MSE performance compared to the MSE performance of estimation based on fine quantization measurements.

The MCRB derived in this paper provides a useful tool for analysis of misspecified one-bit quantization. Future work can investigate the expected performance as a function of different quantization parameters, such as quantization offset. Moreover, the MCRB can be used to design optimal time-varying offset or optimal sampling time in non-uniform sampling. Another research directions can focus on exploring the effect of threshold region shift due to misspecified quantization. It can be done via derivation of misspecified Barankin-type bounds and their implementation for misspecified quantized model with oversampling.

## APPENDIX A

### STATISTICS OF QUANTIZED MEASUREMENTS

The expectation of the quantized measurement  $z_n$  can be derived by using (5)-(7) to obtain

$$\mu_n(\boldsymbol{\theta}) \triangleq \mathbb{E}[z_n], \quad (65)$$

where  $\boldsymbol{\mu}(\boldsymbol{\theta}) \triangleq [\mu_1(\boldsymbol{\theta}), \dots, \mu_N(\boldsymbol{\theta})]^T$ ,

$$\begin{aligned} \mu_{n,R}(\boldsymbol{\theta}) &\triangleq \mathbb{E}[z_{n,R}] = \sum_{z_{n,R} \in \{-1,1\}} z_{n,R} p_{z_{n,R};\boldsymbol{\theta}}(z_{n,R};\boldsymbol{\theta}) \\ &= -Q(-q_{n,R}(\boldsymbol{\theta})) + Q(q_{n,R}(\boldsymbol{\theta})) \\ &= 1 - 2Q(-q_{n,R}(\boldsymbol{\theta})), \end{aligned} \quad (66)$$

in which the property  $Q(-x) = 1 - Q(x)$  is used, and similarly

$$\begin{aligned} \mu_{n,I}(\boldsymbol{\theta}) &\triangleq \mathbb{E}[z_{n,I}] = \sum_{z_{n,I} \in \{-1,1\}} z_{n,I} p_{z_{n,I};\boldsymbol{\theta}}(z_{n,I};\boldsymbol{\theta}) \\ &= 1 - 2Q(-q_{n,I}(\boldsymbol{\theta})). \end{aligned} \quad (67)$$

As  $z_{n,R}, z_{n,I} \in \{-1, 1\}$ , it can be concluded that  $\mathbb{E}[z_{n,R}^2] = 1$ , and  $\mathbb{E}[z_{n,I}^2] = 1$ , and therefore

$$\begin{aligned} \mathbb{E}[|z_n|^2] &= \mathbb{E}[z_{n,R}^2 + z_{n,I}^2] = 2, \\ \mathbb{E}[z_n^2] &= \mathbb{E}[z_{n,R}^2 - z_{n,I}^2 + 2j z_{n,R} z_{n,I}] \\ &= 2j \cdot \mu_{n,R}(\boldsymbol{\theta}) \mu_{n,I}(\boldsymbol{\theta}), \end{aligned} \quad (68)$$

where the last equality in (68) is obtained because  $z_{n,R}$  and  $z_{n,I}$  are uncorrelated.

## APPENDIX B

### PROOF OF PROPOSITION 1

The search parameter  $\varphi'$  is a value in a finite grid with  $K$  possible values. For a grid parameter  $\varphi'$ , the correlator inside the argument in (53) is

$$c(\mathbf{a}(\varphi'), \mathbf{x}) = \sum_{n=1}^N a_n^*(\varphi') x_n, \quad (69)$$

where the  $n$ -th element in the summation in (69) results in

$$\begin{aligned} a_n^*(\varphi') x_n &= (a_{n,R}(\varphi') - j a_{n,I}(\varphi')) (x_{n,R} + j x_{n,I}) \\ &= (x_{n,R} a_{n,R}(\varphi') + x_{n,I} a_{n,I}(\varphi')) \\ &\quad + j (x_{n,I} a_{n,R}(\varphi') - x_{n,R} a_{n,I}(\varphi')). \end{aligned} \quad (70)$$

As the real and imaginary parts  $x_{n,R}$  and  $x_{n,I}$  satisfy  $x_{n,R}, x_{n,I} \in \mathbb{R}$ , the computational cost of (70) results in 4 multiplications and 2 additions, with cost  $6C_{op}$ .

The correlator  $c(\mathbf{a}(\varphi'), \mathbf{z})$  can be defined similarly to (69) with the quantized measurements  $\mathbf{z}$ . The  $n$ -th element in the summation of the correlator  $c(\mathbf{a}(\varphi'), \mathbf{z})$  gives four possible results:

$$\begin{aligned} a_n^*(\varphi') z_n &\in \left\{ f_n(\varphi') + j \cdot d_n(\varphi'), d_n(\varphi') - j \cdot f_n(\varphi'), \right. \\ &\quad \left. - d_n(\varphi') + j \cdot f_n(\varphi'), -f_n(\varphi') - j \cdot d_n(\varphi') \right\}, \end{aligned} \quad (71)$$

where

$$\mathbf{f}(\varphi') \triangleq \Re(\mathbf{a}(\varphi')) + \Im(\mathbf{a}(\varphi')) \quad (72)$$

and

$$\mathbf{d}(\varphi') \triangleq \Re(\mathbf{a}(\varphi')) - \Im(\mathbf{a}(\varphi')), \quad (73)$$

because  $z_{n,R}, z_{n,I} \in \{-1, 1\}$ . The four possible terms in (71) are evaluated using additions or subtractions (without multiplications) in the elements of (72) and (73). Specifically, the computational cost of (71) is four additions/subtractions to yield the values  $\{\pm f_n(\varphi'), \pm d_n(\varphi')\}$ . Thus, the possible values in (71) can be evaluated in cost of  $4C_{op}$ .

The computational cost to evaluate each possible result of  $a_n^*(\varphi')z_n$  for every quantized sample  $z_n$ ,  $n = 1, \dots, N$ , and each grid parameter  $\varphi'$  is therefore  $4C_{op}NK$ . Those computations can be executed once in an offline procedure and saved in a look-up table. Thus, those computations are negligible in terms of computational cost.

To evaluate the complex summations in the correlators (69) and  $c(\mathbf{a}(\varphi'), \mathbf{z})$ ,  $2(N-1)$  additions are required. Two additional multiplications and one sum are required to evaluate the squared absolute values of the correlators (69) and  $c(\mathbf{a}(\varphi'), \mathbf{z})$ .

To summarize, the computational costs for evaluating the squared absolute values of the correlators  $c(\mathbf{a}(\varphi'), \mathbf{z})$  and (69) for each grid parameter  $\varphi'$  are

$$\begin{aligned} C_{\mathbf{z}} &= (2(N-1) + 3) C_{op}K \\ &= (2N+1) C_{op}K \end{aligned} \quad (74)$$

and

$$\begin{aligned} C_{\mathbf{x}} &= C_{op} (6N + 2(N-1) + 3) K \\ &= C_{op} (8N + 1) K, \end{aligned} \quad (75)$$

respectively. The reduction in computational complexity obtained by using one-bit measurements instead of fine quantization measurements is given by the ratio of (74) and (75), which gives (55).

## REFERENCES

- [1] R. H. Walden, "Analog-to-digital converter survey and analysis," *IEEE J. Sel. Areas Commun.*, vol. 17, no. 4, pp. 539–550, 1999.
- [2] M. Verhelst and A. Bahai, "Where analog meets digital: Analog to information conversion and beyond," *IEEE Solid-State Circuits Mag.*, vol. 7, no. 3, pp. 67–80, 2015.
- [3] G. Jacovitti and A. Neri, "Estimation of the autocorrelation function of complex Gaussian stationary processes by amplitude clipped signals," *IEEE Trans. Inf. Theory*, vol. 40, no. 1, pp. 239–245, 1994.
- [4] J. Mo, P. Schniter, and R. W. Heath, "Channel estimation in broadband millimeter wave MIMO systems with few-bit ADCs," *IEEE Trans. Signal Process.*, vol. 66, no. 5, pp. 1141–1154, 2017.
- [5] K. Roth and J. A. Nossek, "Achievable rate and energy efficiency of hybrid and digital beamforming receivers with low resolution ADC," *IEEE J. Sel. Areas Commun.*, vol. 35, no. 9, pp. 2056–2068, 2017.
- [6] P. T. Boufounos and R. G. Baraniuk, "1-bit compressive sensing," in *42nd Annual Conference on Information Sciences and Systems*, 2008, pp. 16–21.
- [7] A. Gokceoglu, E. Björnson, E. G. Larsson, and M. Valkama, "Spatio-temporal waveform design for multiuser massive MIMO downlink with 1-bit receivers," *IEEE J. Sel. Topics Signal Process.*, vol. 11, no. 2, pp. 347–362, 2017.
- [8] Y. Li, C. Tao, G. Seco-Granados, A. Mezghani, A. L. Swindlehurst, and L. Liu, "Channel estimation and performance analysis of one-bit massive MIMO systems," *IEEE Trans. Signal Process.*, vol. 65, no. 15, pp. 4075–4089, 2017.
- [9] C. Mollen, J. Choi, E. G. Larsson, and R. W. Heath, "Uplink performance of wideband massive MIMO with one-bit ADCs," *IEEE Trans. Wireless Commun.*, vol. 16, no. 1, pp. 87–100, 2016.
- [10] D. Ma, N. Shlezinger, T. Huang, Y. Liu, and Y. C. Eldar, "Bit constrained communication receivers in joint radar communications systems," in *IEEE International Conference on Acoustics, Speech and Signal Processing (ICASSP)*, 2021, pp. 8243–8247.
- [11] N. Shlezinger, R. J. G. van Sloun, I. A. M. Huijben, G. Tsintsadze, and Y. C. Eldar, "Learning task-based analog-to-digital conversion for MIMO receivers," in *IEEE International Conference on Acoustics, Speech and Signal Processing (ICASSP)*, 2020, pp. 9125–9129.
- [12] L. T. N. Landau and R. C. de Lamare, "Branch-and-bound precoding for multiuser MIMO systems with 1-bit quantization," *IEEE Wireless Commun. Lett.*, vol. 6, no. 6, pp. 770–773, 2017.
- [13] L. Landau, M. Dörpinghaus, and G. P. Fettweis, "1-bit quantization and oversampling at the receiver: Communication over bandlimited channels with noise," *IEEE Commun. Lett.*, vol. 21, no. 5, pp. 1007–1010, 2017.
- [14] Z. Shao, R. C. de Lamare, and L. T. N. Landau, "Iterative detection and decoding for large-scale multiple-antenna systems with 1-bit ADCs," *IEEE Wireless Commun. Lett.*, vol. 7, no. 3, pp. 476–479, 2018.
- [15] M. Stein, S. Bar, J. A. Nossek, and J. Tabrikian, "Performance analysis for pilot-based 1-bit channel estimation with unknown quantization threshold," in *IEEE International Conference on Acoustics, Speech and Signal Processing (ICASSP)*, 2016, pp. 4353–4357.
- [16] M. Stein, S. Bar, J. A. Nossek, and J. Tabrikian, "Performance analysis for channel estimation with 1-bit ADC and unknown quantization threshold," *IEEE Trans. on Signal Process.*, vol. 66, no. 10, pp. 2557–2571, 2018.
- [17] T. M. Lok and V. K. W. Wei, "Channel estimation with quantized observations," in *IEEE International Symposium on Information Theory*, 1998.
- [18] O. Dabeer and U. Madhoo, "Channel estimation with low-precision analog-to-digital conversion," in *IEEE International Conference on Communications*, 2010, pp. 1–6.
- [19] A. Host-Madsen and P. Handel, "Effects of sampling and quantization on single-tone frequency estimation," *IEEE Trans. Signal Process.*, vol. 48, no. 3, pp. 650–662, 2000.
- [20] O. Bar-Shalom and A. J. Weiss, "DOA estimation using one-bit quantized measurements," *IEEE Trans. Aerosp. Electron. Syst.*, vol. 38, no. 3, pp. 868–884, 2002.
- [21] J. Choi, J. Mo, and R. W. Heath, "Near maximum-likelihood detector and channel estimator for uplink multiuser massive MIMO systems with one-bit ADCs," *IEEE Trans. Commun.*, vol. 64, no. 5, pp. 2005–2018, 2016.
- [22] R. Deng, J. Zhou, and W. Zhang, "Bandlimited communication with one-bit quantization and oversampling: Transceiver design and performance evaluation," *IEEE Trans. Commun.*, vol. 69, no. 2, pp. 845–862, 2021.
- [23] Z. Shao, L. T. N. Landau, and R. C. de Lamare, "Sliding window based linear signal detection using 1-bit quantization and oversampling for large-scale multiple-antenna systems," in *IEEE Statistical Signal Processing Workshop (SSP)*, 2018, pp. 183–187.
- [24] A. B. L. B. Fernandes, Z. Shao, L. T. N. Landau, and R. C. de Lamare, "Multiuser-MIMO systems using comparator network-aided receivers with 1-bit quantization," *IEEE Trans. Commun.*, vol. 71, no. 2, pp. 908–922, 2023.
- [25] C. Mollén, J. Choi, E. G. Larsson, and R. W. Heath, "One-bit ADCs in wideband massive MIMO systems with OFDM transmission," in *IEEE International Conference on Acoustics, Speech and Signal Processing (ICASSP)*, 2016, pp. 3386–3390.
- [26] J. Max, "Quantizing for minimum distortion," *IRE Trans. Inf. Theory*, vol. 6, no. 1, pp. 7–12, 1960.
- [27] D. H. N. Nguyen, "Neural network-optimized channel estimator and training signal design for MIMO systems with few-bit ADCs," *IEEE Signal Process. Lett.*, vol. 27, pp. 1370–1374, 2020.
- [28] A. Doshi and J. G. Andrews, "One-bit mmWave MIMO channel estimation using deep generative networks," *IEEE Wireless Commun. Lett.*, vol. 12, no. 9, pp. 1593–1597, 2023.
- [29] E. Balevi, A. Doshi, A. Jalal, A. Dimakis, and J. G. Andrews, "High dimensional channel estimation using deep generative networks," *IEEE J. Sel. Areas Commun.*, vol. 39, no. 1, pp. 18–30, 2020.
- [30] S. Gao, P. Dong, Z. Pan, and G. Y. Li, "Deep learning based channel estimation for massive MIMO with mixed-resolution ADCs," *IEEE Commun. Lett.*, vol. 23, no. 11, pp. 1989–1993, 2019.
- [31] M. Y. Takeda, A. Klautau, A. Mezghani, and R. W. Heath, "MIMO channel estimation with non-ideal ADCs: Deep learning versus GAMP," in *IEEE 29th International Workshop on Machine Learning for Signal Processing (MLSP)*, 2019, pp. 1–6.

- [32] H. Cramér, *Mathematical Methods of Statistics*. Princeton, NJ, USA, Princeton Univ. Press, 1946.
- [33] C. R. Rao, "Information and accuracy attainable in the estimation of statistical parameters," *Bull. Calcutta Math. Soc.*, vol. 37, pp. 81–91, 1945.
- [34] Z. Shao, L. T. N. Landau, and R. C. De Lamare, "Channel estimation for large-scale multiple-antenna systems using 1-bit ADCs and oversampling," *IEEE Access*, vol. 8, pp. 85 243–85 256, 2020.
- [35] A. Genz and F. Bretz, *Computation of Multivariate Normal and t Probabilities*, 1st ed. Springer Publishing Company, Incorporated, 2009.
- [36] T. Miwa, A. J. Hayter, and S. Kuriki, "The evaluation of general non-centred orthant probabilities," *Journal of the Royal Statistical Society. Series B (Statistical Methodology)*, vol. 65, no. 1, pp. 223–234, 2003.
- [37] N. Zhongren and B. Kedem, "On normal orthant probabilities," *Chinese Journal of Applied Probability and Statistics*, vol. 15, no. 3, pp. 262–275, 1999.
- [38] M. S. Stein, "Performance analysis for time-of-arrival estimation with oversampled low-complexity 1-bit A/D conversion," in *IEEE International Conference on Acoustics, Speech and Signal Processing (ICASSP)*, 2017, pp. 4491–4495.
- [39] M. Schluter, M. Dörpinghaus, and G. P. Fettweis, "Bounds on channel parameter estimation with 1-bit quantization and oversampling," in *IEEE 19th International Workshop on Signal Processing Advances in Wireless Communications (SPAWC)*, 2018, pp. 1–5.
- [40] M. Stein, A. Mezghani, and J. A. Nossek, "A lower bound for the Fisher information measure," *IEEE Signal Process. Lett.*, vol. 21, no. 7, p. 796–799, Jul. 2014. [Online]. Available: <http://dx.doi.org/10.1109/LSP.2014.2316008>
- [41] H. White, "Maximum likelihood estimation of misspecified models," *Econometrica*, vol. 50, pp. 1–25, 1982.
- [42] —, *Estimation, Inference and Specification Analysis*. Cambridge University Press, 1996.
- [43] Y. Noam and J. Tabrikian, "Marginal likelihood for estimation and detection theory," *IEEE Trans. Signal Process.*, vol. 55, no. 8, pp. 3963–3974, 2007.
- [44] Q. H. Vuong, "Cramér–Rao bounds for misspecified models," *Div. of the Humanities and Social Sci., California Inst. of Technol., Pasadena, CA, USA*, 1986.
- [45] C. D. Richmond and L. L. Horowitz, "Parameter bounds on estimation accuracy under model misspecification," *IEEE Trans. Signal Process.*, vol. 63, no. 9, pp. 2263–2278, 2015.
- [46] —, "Parameter bounds under misspecified models," *Proc. Conf. Signals, Systems and Computers (Asilomar)*, pp. 176–180, 2013.
- [47] S. Fortunati, F. Gini, M. S. Greco, and C. D. Richmond, "Performance bounds for parameter estimation under misspecified models fundamental findings and applications," *IEEE Signal Process. Mag.*, vol. 34, no. 6, pp. 142–157, 2017.
- [48] Z. Shao, L. T. N. Landau, and R. C. de Lamare, "Dynamic oversampling for 1-bit ADCs in large-scale multiple-antenna systems," *IEEE Trans. Commun.*, vol. 69, no. 5, pp. 3423–3435, 2021.
- [49] E. Gilbert, "Increased information rate by oversampling," *IEEE Trans. Inf. Theory*, vol. 39, no. 6, pp. 1973–1976, 1993.
- [50] L. T. N. Landau, M. Dörpinghaus, R. C. de Lamare, and G. P. Fettweis, "Achievable rate with 1-bit quantization and oversampling using continuous phase modulation-based sequences," *IEEE Trans. Wireless Commun.*, vol. 17, no. 10, pp. 7080–7095, 2018.
- [51] S. Krone and G. Fettweis, "Communications with 1-bit quantization and oversampling at the receiver: Benefiting from inter-symbol-interference," in *IEEE 23rd International Symposium on Personal, Indoor and Mobile Radio Communications - (PIMRC)*, 2012, pp. 2408–2413.
- [52] T. Koch and A. Lapidoth, "Increased capacity per unit-cost by oversampling," in *IEEE 26-th Convention of Electrical and Electronics Engineers in Israel*, 2010, pp. 000 684–000 688.
- [53] S. Shamai, "Information rates by oversampling the sign of a bandlimited process," *IEEE Trans. Inf. Theory*, vol. 40, no. 4, pp. 1230–1236, 1994.
- [54] A. Eamaz, K. V. Mishra, F. Yeganegi, and M. Soltanalian, "UNO: Unlimited sampling meets one-bit quantization," *IEEE Trans. Signal Process.*, vol. 72, p. 997–1014, Jan. 2024.
- [55] S. Bender, M. Dörpinghaus, and G. Fettweis, "On the achievable rate of bandlimited continuous-time 1-bit quantized AWGN channels," in *IEEE International Symposium on Information Theory (ISIT)*, 2017, pp. 2083–2087.
- [56] A. V. Oppenheim, A. S. Willsky, and S. H. Nawab, *Signals & systems (2nd ed.)*. USA: Prentice-Hall, Inc., 1996.
- [57] N. E. Rosenthal and J. Tabrikian, "The misspecified Cramér–Rao bound for DOA estimation with one-bit quantized data," in *IEEE International Conference on Acoustics, Speech and Signal Processing (ICASSP)*, 2025.
- [58] S. Fortunati, F. Gini, and M. S. Greco, "The misspecified Cramér–Rao bound and its application to scatter matrix estimation in complex elliptically symmetric distributions," *IEEE Trans. Signal Process.*, vol. 64, no. 9, 2016.
- [59] O. Aharon and J. Tabrikian, "A class of Bayesian lower bounds for parameter estimation via arbitrary test-point transformation," *IEEE Trans. Signal Process.*, vol. 71, pp. 2296–2308, 2023.
- [60] I. G. Abrahamson, "Orthant probabilities for the quadrivariate normal distribution," *The Annals of Mathematical Statistics*, vol. 35, no. 4, pp. 1685–1703, 1964.
- [61] M. C. Cheng, "The orthant probabilities of four Gaussian variates," *The Annals of Mathematical Statistics*, vol. 40, no. 1, pp. 152–161, 1969.
- [62] A. Genz and F. Bretz, "Comparison of methods for the computation of multivariate t probabilities," *Journal of Computational and Graphical Statistics*, vol. 11, no. 4, pp. 950–971, 2002.
- [63] H. L. Van Trees, *Optimum Array Processing: Part IV of Detection, Estimation, and Modulation Theory*. John Wiley & Sons, 2004.